Ultrafast carrier dynamics in QD semiconductor optical amplifiers

(numerical simulations and pump-probe experiment)

Miljan Dašić
Student of the first level studies
Faculty of electrical engineering
Belgrade, Serbia
miljandasic@yahoo.com

Abstract— **The aim of this project is to examine relevant carrier (electrons/holes/photons) dynamics of a Quantum Dot Semiconductor Optical Amplifier (QD SOA) using pump-probe experiment and programming numerical simulations of a QD SOA. The speed of the carrier dynamics in a QD SOA is ultrafast because the transitions happen at picosecond timescale. We assume Auger dominated and phonon assisted mechanisms. Greater importance of Auger processes was obtained, which is a common result in the literature [3], [8]. Standard transitions between energy levels of a QD were used with the addition of the direct transition between Wetting Layer and Ground State. Pump-probe experiment has been performed. The gain and phase dynamics were time resolved for different currents. Three-exponential fit of those results was done and the timescales were exctracted as functions of the current.**

Key words-Quantum Dot; Semiconductor optical amplifier; carriers; dynamics; pump-probe

I. INTRODUCTION

Understanding of the ultrafast dynamics of semiconductor materials is extremely important in order to develop and improve next generation photonic sources. Ultrafast pump-probe measurements have been used to experimentally investigate the gain and phase recovery dynamics of QD SOAs - [1], [2], [3]. Main part of a QD SOA is optical cavity (active region) that is made between p-type and n-type layers. Essencialy this device is a P-N junction because the band structure of an inverse populated P-N junction is the best structure for stimulated emission of light. In order to achieve the inverse population a SOA is pumped by injected current. The amplification happens by stimulated emission. The gain G of an QD SOA is its most important parameter. It is defined as the ratio of output over input power. A QD SOA consists of a large number of Quantum Dots grown in the Wetting Layer which is made of Quantum Wells. A simple Quantum Mechanical model of a QD would be a potential pit with finite height, therefore the energy levels possible into QD are discrete and depend on the depth of that potential pit, which means they depend on the size of a QD. Because of that, we use energy broadening in the model. Carrier dynamics includes radiative and non-radiative recombinations. In radiative recombinations, electron-hole pair is recombined with the presence of a photon which can be emitted or apsorbed. In nonradiative recombinations, photons are not present. Main radiative processes are spontaneous emission, amplified emission and absorption. Nonradiative processes are phonon assisted and Auger mediated recombinations. The transition between two states can be either a capture or an escape. If a carrier goes from higher level to lower, it is called capture and the transition from lower to higher energy level is an escape.

II. MODEL

The carriers we are dealing with are electrons in the conduction band (CB) and holes in the valence band (VB). Photons are created in recombine processes between electrons and holes from corresponding energy levels. We assume the existence of three different energy states for both CB and VB. The energy lowest is Ground State(GS), Excited State(ES) is higher energy state of excited carriers and Wetting layer(WL) corresponds to the reservoir of particles which is pumped by the current that supplies the power to the device.

A real QD SOA device is built of a huge number of quantum dots. Therefore, we divide GS and ES energy levels into ensembles of quantum dots with given energy and WL is one constant energy level, similar to Moreno et al[7]. This division gives us a model of a device consisting of different quantum dots, with different sizes and potential barriers and also leads to inhomogenous broadening of the emitted photons. The energy range of the simulation is between 0.919 and 1.18 eV. NumberSteps is the number of pieces that we are using. It was shown that resolution of 150 pieces is enough for good accuracy. Energy step is calculated as:

$$E_{step} = \frac{E_{\max} - E_{\min}}{NumberSteps}$$

The meaning of the broadening shown in Figure 1. is that the device should give that shape of the spectrum as the output, therefore we set the resolutions for each energy piece. The distribution is Gaussian with a full width half maximum (FWHM) of 35 meV for both GS and ES, like in [7]. We have chosen the peaks of the emission: $\lambda_{GS} = 1300nm$ and $\lambda_{ES} = 1165nm$

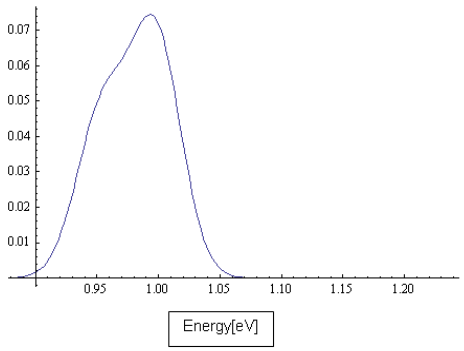

Figure 1. Inhomogenuous broadening of the GS and ES

The resolution of k-th part of the GS is calculated as a ratio of those two integrals of Gaussian distribution. The value of resolution is between 0 and 1 because it measures the ratio of integration over E_{step} interval around given energy divided by the integration over full energy scan.

$$resGS(k) = \frac{\int_{E_{GS}(k)-E_{step}/2}^{E_{GS}(k)+E_{step}/2} e^{\frac{-(x-E_{GSpeak})^2}{2\sigma^2}} dx}{\int_{E_{\min}}^{E_{\max}} e^{\frac{-(x-E_{GSpeak})^2}{2\sigma^2}} dx}$$

For the ES it is simmilar and the ratio of those two integrals is multiplied by 1.5. The Lorentzian function is used to describe that emission does not happen only for certain energy difference, but it can happen between k-th and j-th piece with the probability given by narrow Lorentzian distribution, meaning that photons of k-th energy can be produced after k-th and j-th piece recombine.

$$L(k)(y) = \frac{\Gamma}{\pi[\Gamma^2 + (E_{GS}(k) - E_{GS}(y))^2]}$$

where Γ is factor of homogenous broadening: Γ = 7.5 meV.

As usual in this area, the heart of the model are ratio equations. The ratio equations in this project are similar to those in [7] and [8] meaning that electron and hole equations are like in [8] and photon equations are like in [7] with the difference that in our model both Auger and phonon assisted processes are included. Also, a direct transition between WL and GS is added as additional connection between the levels that was not considered in [7] and [8]. The carrier dynamics equations are considered separately for electrons, holes and photons, but they are all coupled. Basically, we are solving 1 equation for electron WL, 1 for hole WL, NumberSteps*6 (for electron and hole GS and ES and for GS and ES photons) which means 902 coupled differential equations in total. GS photons are photons got in the radiative recombinations between the ground states of CB and VB, and ES photons are got in the processes between the excited states of CB and VB.

The GS photons equation (for ES photons it is simmilar) for i-th energy slice is:

$$\frac{\partial \mathrm{Pg(i)}}{\partial \mathrm{t}} = \frac{2\beta}{NumberSteps} \sum_{k=1}^{NumberSteps} \frac{res(k)\cdot hNg(k)\cdot eNg(k)}{\tau_r} + 2bPg(i) \sum_{k=1}^{NumberSteps} L(k)(i)\cdot res(k)\cdot \left(hNg(k)+eNg(k)-1\right) - \frac{Pg(i)}{\tau_\varphi}$$

Equation for WL of electrons and holes:

$$\frac{\partial Nw}{\partial t} = J - \sum_{k=1}^{NumberStes} \frac{res(k)\cdot Nw^{\alpha}\cdot(2-Ne(k))}{\tau we} + \sum_{k=1}^{NumberSteps} \frac{Ne(k)^{\alpha}}{\tau EW(k)} + \sum_{k=1}^{NumberStes} \frac{Ng(k)^{\alpha}}{\tau GW(k)} - \sum_{k=1}^{NumberStes} \frac{res(k)\cdot Nw^{\alpha}\cdot(1-Ng(k))}{\tau wg} - \left(\frac{1}{\tau_r} + \frac{1}{\tau nr}\right)\cdot Nw\cdot Nw^{*}$$

where res(k) corresponds to resES(k) or resGS(k) and Nw* means the opposite carrier's WL density.

The electron/hole equation for i-th energy slice of ES (for GS it is simmilar) is

$$\frac{\partial Ne(i)}{\partial t} = \frac{Nw^{\alpha}\cdot(2-Ne(i))}{\tau we} - \frac{Ne^{\alpha}(i)\cdot Nw}{\tau EW[i]} - \frac{Ne^{\alpha}(i)\cdot(1-Ng(i))}{\tau eg} + \frac{Ng^{\alpha}(i)\cdot(2-Ne(i))}{\tau GE[i]} - b\left(Ne(i)+Ne^{*}(i)-1\right)\sum_{k=1}^{NumberSteps} L(k)(i)\cdot res(k)\cdot Pe(k) - \left(\frac{1}{\tau_r} + \frac{1}{\tau nr}\right)Ne(i)\cdot Ne^{*}(i)$$

where Nw, Ne and Ng are the normalized carrier densities of the WL, ES and GS, respectively. Photon populations of GS and ES are Pg and Pe, respectively. The index (i) or (k) counts the number of i-th or k-th energy slice. In the program there is (t) index which means a function of time, but we skip it here. Important feature of the rate equation models is that the dynamics of the capture/escape processes and the recombination processes can be expressed using the parameter α which can take the integer values 1 or 2 depending on the dominant process we want to include into the model equations. The parameterization for the capture/escape terms is like in[8]:

$\alpha = 1$ corresponds to phonon assisted process and $\alpha = 2$ corresponds to an Auger mediated process. In Auger processes there is a collision of two carriers, therefore density is squared. Terms (1-Ng) and (2-Ne) are Pauli blocking factors, meaning that maximal value of normalized densities of carriers in GS and ES are limitied to 1 and 2, respectively. The ES is two times more dense, therefore we use factor 2. The physical interpretation is that saturation of GS (Ng = 1) stops further fill of GS and because of that, term (1-Ng) in the capture processes to GS becomes zero, so further filling is blocked because GS is already full. This type of blocking factor is not used for the WL

because it has constantly being refilled by the current J, so Nw can take arbitrary high value. A serious numerical model has to include huge number of parameters in order to describe the system better. Using form τ_{ab} we represent the carrier lifetime due to the transition from energy level a to energy level *b*. Those parameters are of great importance because the essence of the whole simulation is to calculate the time response of the QD SOA, solving the system of coupled equations in time domain. Every process that happens has its average lifetime, for electrons and for holes separately. It is possible to get fine results only by using appropriate values for those time parameters. For example, carrier lifetime of 10 ps means that in average 10 picoseconds will go until that carrier performs the transition. We assume that capture times are constant and using formula

$$\tau_{esc} = \tau_{cap} e^{\frac{\Delta E}{k_B T}}$$

we calculate the escape times.

III. Simulation

Presented model is implemented in Mathematica. First part of the code consists of the constants, parameters and the calculations for the broadening (Gaussian integrals and Lorentzian function). After that, equations are written and all initial conditions set to zero. The system of the equations is solved using NDSolve (StiffnessSwitching Method).

The gain temporal changes of an QD SOA are of the key importance for its performance, so we examine it, in the simulation and using pump-probe experiment. In the simulation, gain is calculated using photon populations.

IV. Pump-Probe Experiment

A. General idea

Pump–probe measurements are used to obtain information on ultrafast phenomena. The general principle goes like this. A sample gets hit by a pump beam, which causes a perturbation in the sample. After an adjustable time delay that is controlled using time delay stage, a probe pulse hits the sample and its transmission is measured. By measuring the probe signal as a function of the time delay, it is possible to obtain information on the decay of the pump generated excitation. The temporal resolution of the experiment is limited only by the pulse duration, so we need the laser that generates ultrashort pulses.

Pump pulse is used to provide initial depletion of the amplifier, Non-equilibrium carrier distribution results in changed transmittance (gain/absorption and refractive index), which are affecting following probe pulse, changing its amplitude and phase. Carriers returning then to equilibrium state are affected by different radiative and non-radiative processes such as phonon or Auger assisted recombination. Such processes affect recovered time traces, so by proper choice of experimental conditions it is possible to pinpoint processes governing dynamics in the device.

Detection part of the system has to be also more complicated a the pump and probe beams cannot be spatially separated. In simplest case they can be cross-polarized, but due to the strong anisotropy of QD's this type of measurement won't provide full information on the carrier relaxation. In addition both beams have often the same wavelength and intensity of probe pulses is very low, on the level of few 100's of nW. The solution is provided by heterodyne probe detection, based on a fact that overlapping two waves with high frequencies f_1 and f_2 will produce a beating signal with a small frequency Δf equal to the difference of frequencies of original waves.

Heterodyning is commonly used in many types of detection systems as it allows detecting weak, high frequency signals using slow detectors of average sensitivity – most common example is a radio. Usually one of the signals is produced by local oscillator (LO) of known frequency and the other has external source e.g. in case of radio it is input amplifier, or laser beam passing through the tested device.

These two signals are in our case reference and probe pulses, whose frequencies are shifted by f_1=79MHz and f_2=80MHz, respectively. As amplitude and phase between reference pulses are stable, both amplitude and phase of the beating signal depend only on the probe beam. Characterization of this beating signal provides information about device gain and refractive index properties in function of delay between pump and probe pulses.

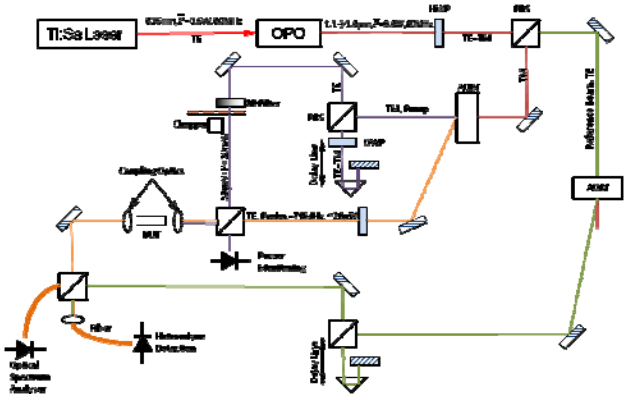

Figure 2. Pump-probe optics schematic

B. Technical details about the experiment

Power of the pump and probe beam (before coupling to the waveguide) was 500 µW and 20 µW. Pump probe always has higher power because it perturbates the system and probe is used for collecting the data about that perturbation. We have used Single Color (SC) pump-probe which means that central wavelength of both pump and probe is 1.3 µm. Bandwith of the spectrum had Full Width Half Maximum (FWHM) of 20 nm. Pusle duration was 300 fs which is related to the time resolution of the experiment. Pump and probe beam had the same Transverse Electric (TE) polarization. The experiment was done at the room temperature (sensor was stable showing $\sim 20^{\circ} C$). In pump-probe experiments it is possible to pump and probe both GS and ES. We have used pumping and probing of GS only.

The main difficulties in the pump-probe and in device characterization were to align every mirror and optical element proper and to couple enough amount of light into the Single Mode Fiber (SMF) in order to perform spectrum analysis or some other measurement.

V. Results and Discussion

A. Characterization of the device

The QD SOA device we were using in the experiments has sample number: QD DO1421, It comes from Innolume company. We got the layer of numeruous devices and then the devices were extracted by the employees in fabrication labs. First of all, the device was mounted and put on the optical bench. It was connected to the current source and optical-current characteristic was measured using a powermeter. In the Figure 3. optical-current characteristic of three different QD SOAs grown on the same layer is given.

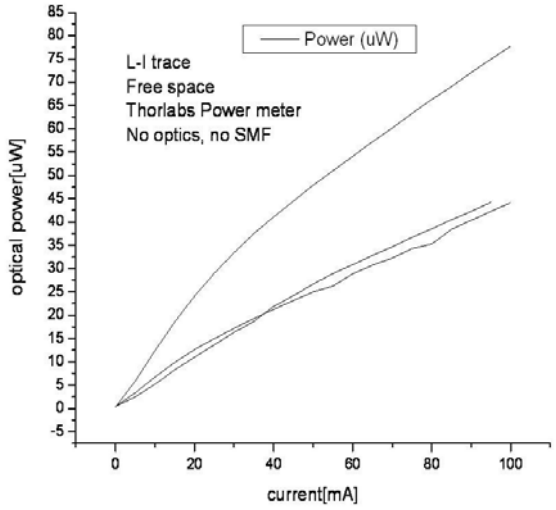

Figure 3. Optical-current characteristic of the SOA-s

There is no treshhold current which means that the devices are not lasers, they act as amplifiers. After we confirmed the devices are amplifiers, the spectrum analysis was performed. For 10mA we notice that only the GS emittes and on 100mA GS is higher but on currents > 100mA, it will go to saturation and the ES starts to rise.

B. One single QD SOA simulation

The simulation of a single QD SOA by solving the model equations has given fine results. The curves are smooth and stable. After turning on the device, stady state is achieved after some time. Stady state means that the carrier densities and photon populations are constant. The time required to achieve stady state extracted from the simulation results is about 20 to 50 picoseconds. It is in a good agreement with the times from the experiment. In the experiment, we first measure the optical-current characteristic to prove that the device is a SOA, and after that, using pump-probe gain and phase recovery are got. The same procedure is in the simulation. First we plot optical-current characteristic which is normalised number of photons (Pg and Pe) as a function of current. In a for loop we change the current and solve the equations for every current. The photons number is taken at phoTime=20ps because that is the time when solutions become stable. We got the saturation of GS emission which happens in the experiment as we can see the saturation of GS on spectrum diagrams. The ES emission increases with the increase of the current and the curve looks similar to those in Figure 3.

The time plots of GS and ES gains were got. We can notice two different regimes – absorption and gain regime, as reported in [3]. The absorption regime happens on low current when inverse population is not achieved. GS absorption was got for simulation current of J=0.5 and ES absorption was got for J=0.9. The gain regime happens on high current when inverse population is achieved. Both GS and ES gain regimes were got for J=5. Comparing the values of GS and ES photons populations in absorption and gain regime, we can conclude that ES is affected by the current changes stronger than GS.

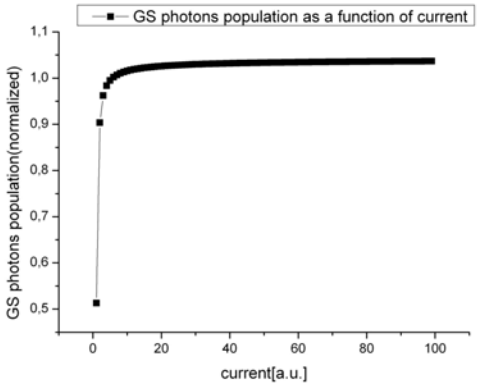

Figure 4. GS photons optical-current characteristic

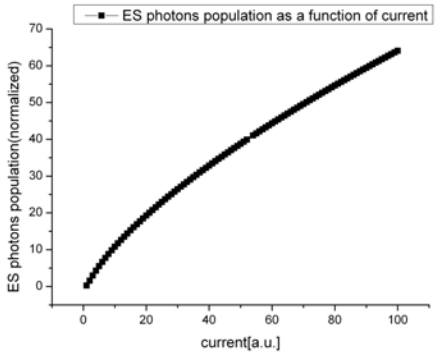

Figure 5. ES photons optical-current characteristic

In Figures 6. and 7. ES photons population is shown with Auger processes and without them, respectively. Without Auger processes we didn't get stady state in 50ps time range which means that the device is not stable. When we include Auger processes, ES photons population goes to stady state after ~20ps which is reasonable time.

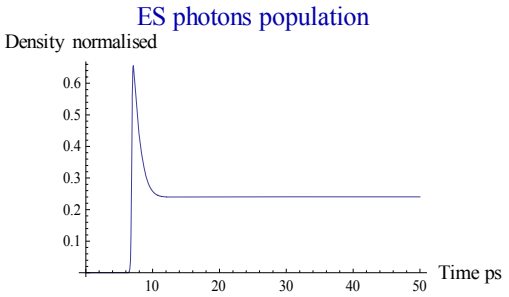

Figure 6. ES photons population time resolved (Auger included)

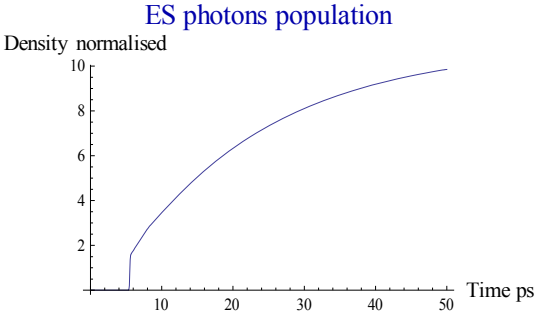

Figure 7. ES photons time resolved (Auger excluded)

C. *Ensembles of Quantum Dots on different energies*

The results of the simulation that considers different energy levels and broadening of the light are shown. The comparison of the results with direct transition WL←→GS and without that transition is made. We were using different timescales, 200ps for the simulation with WL←→GS and 1000 ps for the simulation without that transition because it was expected to get faster response with additional process. As we can see in those plots, additional process does not make a big difference in both the stable values and tmes needed for achieving stable response. The only difference is that results with WL←→GS are more compact for GS electrons and holes, meaning that time resolved carrier densities for different energy levels within GS more converge to one curve than in the model without additional transition where divergence of the results is higher. More expected result is to get divergence because different energy levels should have different densities of carriers because escape lifetimes directly depend on the energy differences between the levels.

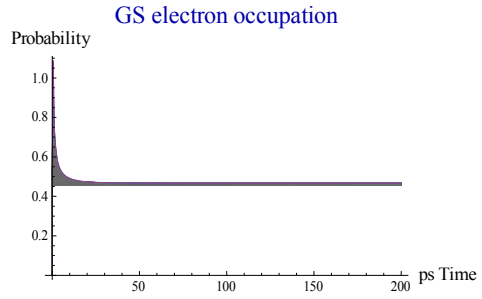

Figure 8. GS electron occupation time resolved (with WL←→GS)

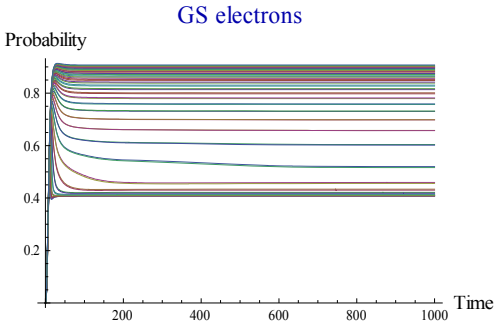

Figure 9. GS electron occupation time resolved (without WL←→GS)

D. *Results of the pump-probe experiment*

In the pump-probe experiment time delay between pump and probe beam is changing and the gain and phase are measured as functions of the time delay. This gives us the time recovery of the device. Depending on the current that is injected into the device, there are two different regimes – apsorbtion and gain.

The absorption regime plot is given for 10mA and gain regime plot is given for 50mA.

On the lower current inverse population is not achieved. When pump beam enters the cavity of the device it gets apsorbed. An electron from the VB apsorbs a photon of the pump beam and goes to the CB leaving a hole in the VB. This leads to higher number of relevant carriers in both bands. When the probe beam arrives after the time delay we set, there are conditions for the emission and gain increases, recovers to the constant level in the stady state. On the other side, in the gain regime inverse population is achieved because of the higher current. When the pump beam arrives the gain instantenuously increases because the conditions for the stimulated emission are already satisfied. As the time delay increases, gain changes decrease because the probe beam sees lower inverse population due to the emission that goes all the time. After some amount of time device goes to stady state and gain changes keep being constant when time delay increases. It is obvious that recovery time in the absorption regime is higher than in the gain regime. It indicates that apsorbtion processes are the slowest component in the ultrafast carrier dynamics.

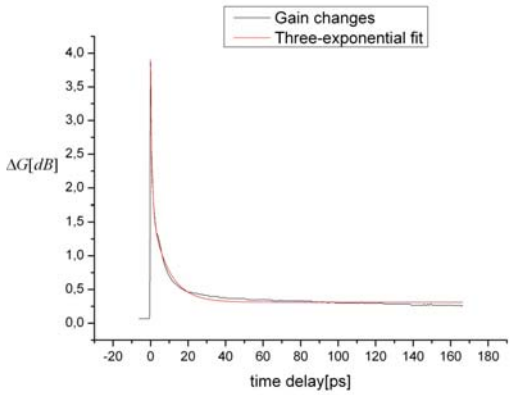

Figue 10. Gain changes on 50 mA

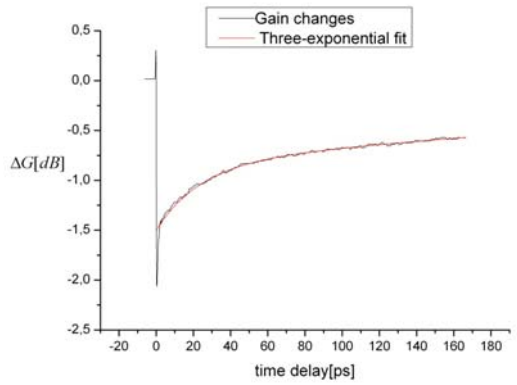

Figure 11. Gain changes on 10 mA

The three-exponential decay fit is performed using Origin's fitting tool and ExpDecay3 function. It reads:

$$y = y_0 + A_1 e^{-\frac{x-x_0}{t1}} + A_2 e^{-\frac{x-x_0}{t_2}} + A_3 e^{-\frac{x-x_0}{t_3}}$$

where A1, A2 and A3 are the amplitudes of exponential decay components and t1, t2 and t3 are time constants in those exponential decays. The three exponential fit indicates that there are three components of carrier dynamics in a QD SOA – ultrafast, medium and slow.

VI. Conclusions and Further Work

Pump-probe measurements of gain and phase recoveries of a QD SOA have been performed. The fitting with three-exponential decay is successfull and three different timescales are extracted and ploted as a function of current. The plots are simmilar to the results in [8]. Removing of the Auger processes from the model equations causes slower response and the solutions that do not correspond to the experimental results, therefore we have concluded that they affect the dynamics strongly. Adding the direct transition WL←→GS does not make a big difference in the solutions and for GS it leads to lower divergence of the results, therefore there are not advantages in adding that process to the model equations.

Results of single QD SOA simulations have shown good agreement with the experimental results which means that it is possible to use the ratio equations from this project to model a QD SOA.

When the broadening was introduced, the simulation has become complicated. The main problem is that we need to use large number of parameters with unknown values, so estimations have to be made. All of the model equations are coupled and changing of one parameter (carrier lifetime for a certain process or energy level) strongly affects the solution of the system. In the experiment we extracted three different timescales but it is impossible to connect them to every particular time parameter in the model.

Spectrum plots of carrier densities and photon populations as functions of wavelength have been made but they were not good enough, so there is a huge space of improving the simulation in order to achieve better spectrum characteristics of the light emitted by the QD SOA.

Acknowledgements

I am very thankful to my PhD student mentor Jaroslaw Pulka for his support in the programming in Mathematica and explaining me the model I was using. Also I would like to say many thanks to my supervisor Dr Tomasz Piwonski for his help and explanations about the pump-probe experiment and in general, about the lab work. The UREKA program 2011 funded by Science Fundation Ireland has given me a great chance to experience real scientific work at high class institute, which Tyndall National Institte in Cork (Ireland) definitely is, and I am very thankfull for that.

References

[1] P. Borri, S. Schneider,W. Langbein, and D. Bimberg, "Ultrafast carrier dynamics in InGaAs quantum dot materials and devices," *J. Opt. A:Pure Appl. Opt.*, vol. **8**, pp. S33–S46, 2006.

[2] S. Dommers, V. V. Temnov, U.Woggon, J. Gomis, J. Martinez-Pastor, M. Laemmlin, and D. Bimberg, "Complete ground state gain recovery after ultrashort double pulses in quantum dot based semiconductor optical amplifier," *Appl. Phys. Lett.*, vol. **90**, no. 033508, 2007.

[3] I. O'Driscoll, T. Piwonski, C.-F. Schleussner, J. Houlihan, G. Huyet, and R. J. Manning, "Electron and hole dynamics of InAs/GaAs quantum dot semiconductor optical amplifiers," *Appl. Phys. Lett.*, vol. **91**, no. 071111, 2007.

[4] Piwonski, T., O'Driscoll, I., Houlihan, J., Huyet, G., Manning, R., Uskov, A.: "Carrier capture dynamics of InAs/GaAs quantum dots". Appl. Phys. Lett. **90**(12), 122108 (2007)

[5] Rossetti, M., Markus, A., Fiore, A., Occhi, L., Vélez, C.: "Quantum dot superluminescent diodes emitting at 1.3 μm". IEEE Photonics Technol. Lett. **17**(3), 540–542 (2005)

[6] Saito H., Nishi, K., Kamei, A., Sugou, S.: "Low chirp observed in directly modulated quantum dot lasers". IEEE Photonics Technol. Lett. **12**(10), 1298–1300 (2000)

[7] Moreno P., Rossetti M., Deveaud-Plédran B.,Fiore A.:" Modeling of gain and phase dynamics in quantum dot amplifiers", Opt Quant Electron (2008) **40**:217–226DOI 10.1007/s11082-008-9219-4

[8] Ian O'Driscoll PhD thesis

[9] Kim J., Meuer C., Bimberg D., Eisenstein G.:"Numerical Simulation of Temporal and Spectral Variation of Gain and Phase Recovery in Quantum-Dot Semiconductor Optical Amplifiers", IEEE Joural Of Quantum Electronics, Vol. 46, No. **3**, MARCH 2010